Dynamics of Carbon Dioxide Sorption on Activated-Carbon Particles

Peter G. Gray and Duong D. Do
Dept. of Chemical Engineering, University of Queensland, St Lucia QLD 4072, Australia

A theoretical model comprising the processes of micropore, macropore and surface diffusion was derived and applied to the dynamics of adsorption of CO_2 on a single activated-carbon particle. The effects of a nonlinear isotherm (Langmuir), particle nonisothermality and concentration dependence of the surface diffusivity were also incorporated. The theoretical model was fitted to a preliminary set of adsorption experimental data (two particle sizes, and various temperatures and concentrations) to determine the diffusion coefficients. The validity of the theoretical model was checked by using the model, with fitted diffusivities, to simulate dynamic adsorption curves at conditions different from those of the preliminary fitting data set. These model simulations were found to predict the experimental data in a satisfactory manner.

Introduction

Knowledge of the adsorption of CO_2 on activated carbon is of importance to the design and operation of current and potential future processes. Many gas streams in oil refining, iron/steel and natural gas industries contain significant amounts of CO_2 that needs to be extracted economically. Conversely, in such applications as removal of SO_2 and NO_x from stack gases, CO_2 present in the flue gas can degrade the ability of an adsorbent to remove the toxic species. In both of these cases, where adsorption of CO_2 is either desirable or undesirable, it is necessary to understand the fundamental interactions occurring between CO_2 and the adsorbent. The objective of this work is to describe effectively the dynamics of CO_2 sorption on activated carbon.

There has been extensive research on equilibrium adsorption of CO_2 on activated carbon and coal (Gregg and Sing, 1982) for the purpose of elucidating pore structure and surface area. Very little quantitative information on the dynamics of CO_2 adsorption on carbon particles, however, had been available prior to the work of Andrieu and Smith (1980), who used a bidisperse model of the carbon pore structure, allowing for diffusional transport in the macropore and micropore regions, which was coupled to the equations for a chromatographic column. By using the moments technique, they matched their model to experimentally-determined sorption of CO_2 on BPL activated carbon, thus extracting the macropore and micropore diffusion coefficients and equilibrium constants over a range of temperatures.

The model used by Andrieu and Smith assumed isothermal adsorption conditions. However, it has been shown by Sircar (1981) that, in such systems, sorption dynamics can be highly nonisothermal under certain experimental conditions, particularly when adsorption is fast and heat transfer away from the carbon particles is poor. The experimental arrangement used by Sircar consisted of a bundle of carbon particles (BPL and MSC V) suspended inside a volumetric apparatus, with thermocouples embedded at different positions within the adsorbent pile to measure the carbon temperature. This configuration was found to give adsorption dynamics that were totally controlled by heat transfer through the particle external stagnant film, and attempting to model the data with an isothermal pore diffusion mechanism gave misleading diffusion coefficients. Heat transfer resistance has also been found to affect the values of diffusivities extracted with an isothermal model for the system of CO_2 in 4A and 5A zeolite crystals, measured in a vacuum gravimetric apparatus (Yucel and Ruthven, 1980).

In addition to the sorbate transport through the macropore and micropore regions of activated carbon, it is possible for gases that adsorb significantly to have an additional flux in the sorbed or "surface" phase that is in parallel with the macropore void diffusion mechanism (Yang, 1987). While mo-

---

Correspondence concerning this article should be addressed to D.D.Do.

bility of molecules in the sorbed phase is smaller than that in the macropore void phase, their concentration is much higher, so that significant surface fluxes are possible. Given that most microporous sorbents necessarily promote large sorbed-phase concentrations, it is often important to include a surface diffusion mechanism in theoretical models of sorption dynamics. This was highlighted by Doong and Yang (1986) in their study of the PSA separation of a mixture of $CO_2/H_2/CH_4$, where they found that surface diffusion contributed as much as 50% of the total flux in the pores of their activated-carbon sorbent. The surface flow of carbon dioxide on microporous carbons has also been measured by Carman and Raal (1951), Ash et al. (1963), and Popielawski (1967).

The objective of this article is to develop a useful single-particle model to describe and predict adsorption dynamics of CO_2 on activated carbon. The model includes the mechanisms of macropore, micropore and surface diffusion with a nonlinear isotherm, together with the effects of nonisothermality and surface coverage on particle uptake dynamics. The validity of the model is established by fitting to CO_2/activated-carbon dynamic data obtained by a microbalance technique.

Theoretical Development

The assumptions necessary for formulation of the single-particle dynamic model are:

- The activated-carbon sorbent particle is assumed to have a bidispersed pore-size distribution comprising a microporous solid penetrated throughout a network of larger interconnected pores (macropores). The microporous solid phase is considered to be composed of many minute microparticles (containing the micropores), which can be of various shapes (slab, cylinder, or sphere) but, for model simplicity, are usually assumed to be spherical (Andrieu and Smith, 1980).
- The resistances controlling the sorption dynamics are due to macropore, micropore, and surface (sorbed-phase) diffusion.
- The carbon particle geometry is arbitrary (slab, cylinder, or sphere).
- The macropore and micropore diffusivities are independent of sorbate concentration, but the surface diffusivity is coverage-dependent.
- Adsorption on the macropore surface is negligible compared to the total adsorption capacity.
- Sorption at the pore mouth of the micropore follows an equilibrium isotherm (Langmuir).
- The particle temperature is allowed to vary with sorbate uptake.

Using these assumptions, the mass balance equation for the microsphere may be expressed as:

$$\frac{\partial C_\mu}{\partial t} = \mathfrak{D}(T_P)\,\frac{1}{r_\mu^2}\frac{\partial}{\partial r_\mu}\left(r_\mu^2\,\frac{\partial C_\mu}{\partial r_\mu}\right) \tag{1}$$

with boundary conditions,

$$r_\mu = 0,\quad \frac{\partial C_\mu}{\partial r_\mu} = 0 \tag{1a}$$

$$r_\mu = R_\mu,\quad C_\mu = \frac{C_{\mu s} b(T_P) C}{1 + b(T_P) C} \tag{1b}$$

In formulating the mass balance for the macroscopic particle, it is necessary to take into account the sorbed-phase concentration (coverage, θ) dependency of the surface diffusivity ($\mathfrak{D}_S$). Thus, $\mathfrak{D}_S$ appears within the divergence term of the surface flux as shown in the particle mass balance below.

$$\epsilon_M\frac{\partial C}{\partial t} + (1-\epsilon_M)\frac{\partial \overline{C}_\mu}{\partial t} = \epsilon_M \mathfrak{D}_P(T_P)\,\frac{1}{r^s}\frac{\partial}{\partial r}\left(r^s\,\frac{\partial C}{\partial r}\right) + (1-\epsilon_M)\,\frac{1}{r^s}\frac{\partial}{\partial r}\left(r^s \mathfrak{D}_S(T_P,\theta)\,\frac{\partial \overline{C}_\mu}{\partial r}\right) \tag{2}$$

with boundary conditions,

$$r = 0,\quad \frac{\partial C}{\partial r} = \frac{\partial \overline{C}_\mu}{\partial r} = 0 \tag{2a}$$

$$r = R,\quad \epsilon_M \mathfrak{D}_P(T_P)\left.\frac{\partial C}{\partial r}\right|_R + (1-\epsilon_M)\mathfrak{D}_S(T_P,\theta)\left.\frac{\partial \overline{C}_\mu}{\partial r}\right|_R = k_m(C_b - C|_R) \tag{2b}$$

where $\overline{C}_\mu$ is the volume-average microsphere concentration at particle radial position r and is given by:

$$\overline{C}_\mu = \frac{4\pi \int_0^{R_\mu} r_\mu^2 C_\mu\, dr_\mu}{4\pi \int_0^{R_\mu} r_\mu^2\, dr_\mu} \tag{3}$$

The first term on the left of Eq. 2 represents the adsorbate accumulation in the macropore void, and the second term is accumulation in the microporous solid phase. The two terms on the righthand side of Eq. 2 show the diffusional flux of the sorbate through the macropore void and microporous solid phases.

If the sorption dynamics within a sorbent particle are very fast, then the released heat of adsorption may not be dissipated quickly enough and the temperature of the particle will vary. Consequently the change in temperature will affect the sorption equilibrium and the macropore, micropore and sorbed phase diffusivities. Given the possibility of these nonisothermal effects, it is necessary to include a heat balance for the particle. Heat transfer within the particle is usually much faster than the heat loss through the external stagnant film of the particle. Hence, we can assume that there is no radial temperature distribution in the particle, so that a single, lumped equation adequately describes the particle temperature (Ruthven, 1984). Based on this principle, a heat balance over the particle gives:

$$\rho_P C_P \frac{dT_P}{dt} + \frac{(s+1)h(T_P - T_0)}{R} - \frac{(s+1)(1-\epsilon_M)}{R^{s+1}} \times (-\Delta H)\int_0^R \frac{\partial \overline{C}_\mu}{\partial t}\, r^s dr = 0 \tag{4}$$

where the microsphere accumulation term can be equated with the flux at the surface of the microsphere (derived from Eq. 1):

$$\frac{\partial \overline{C}_\mu}{\partial t} = \mathfrak{D}(T_P)\,\frac{3}{R_\mu}\,\frac{\partial C_\mu}{\partial r_\mu}\bigg|_{R_\mu} \tag{4a}$$

The variables and parameters in the above equations are defined as follows. C is the sorbate concentration in the macropore, C_μ is the sorbate concentration in the microsphere, C_b is the adsorbate concentration in the bulk gas phase, ϵ_M is the macropore porosity, $\mathfrak{D}_P$ is the macropore diffusivity, $\mathfrak{D}$ is the micropore diffusivity, $\mathfrak{D}_S$ is the surface diffusivity, R is the particle radius, R_μ is the microsphere radius, k_m and h are the film mass and heat transfer coefficients, ρ_P and C_P are the particle density and heat capacity, and s is the particle-shape factor ($s=0$, 1 and 2 for slab, cylinder and sphere, respectively).

We define the nondimensional variables and parameters as:

$$A=\frac{C}{C_0}\quad A_b=\frac{C_b}{C_0}\quad A_\mu=\frac{C_\mu}{C_{\mu 0}}\quad \overline{A}_\mu=\frac{\overline{C}_\mu}{C_{\mu 0}} \tag{5a}$$

$$\theta_P=\frac{T_P-T_0}{T_0}\quad x=\frac{r}{R}\quad x_\mu=\frac{r_\mu}{R_\mu}\quad \lambda=b_0C_0 \tag{5b}$$

$$\tau=\frac{(\epsilon_M D_{P0})t}{(\epsilon_M+(1-\epsilon_M)C_{\mu 0}/C_0)R^2}$$

$$\sigma_1=\frac{\epsilon_M}{(\epsilon_M+(1-\epsilon_M)C_{\mu 0}/C_0)}$$

$$\sigma_2=1-\sigma_1 \tag{5c}$$

$$\gamma=\frac{(\epsilon_M+(1-\epsilon_M)C_{\mu 0}/C_0)\mathfrak{D}_0R^2}{\epsilon_M\mathfrak{D}_{P0}R_\mu^2}=\frac{\mathfrak{D}_0/R_\mu^2}{\sigma_1\mathfrak{D}_{P0}/R^2}$$

$$\delta=\frac{(1-\epsilon_M)\mathfrak{D}_{S0}C_{\mu 0}}{\epsilon_M\mathfrak{D}_{P0}C_0}=\frac{\sigma_2\mathfrak{D}_{S0}}{\sigma_1\mathfrak{D}_{P0}} \tag{5d}$$

$$Bi=\frac{k_mR}{\epsilon_M\mathfrak{D}_{P0}};\quad LeBi_h=\frac{hR}{\rho_PC_P\mathfrak{D}_{P0}} \tag{5e}$$

$$\psi=\frac{(1-\epsilon_M)C_{\mu 0}(-\Delta H)}{\rho_PC_PT_0};\quad Q=\frac{\mathfrak{D}_P(T_P)}{\mathfrak{D}_{P0}}=(1+\theta_P)^\beta \tag{5f}$$

$$P=\frac{\mathfrak{D}(T_P)}{\mathfrak{D}_0}=\exp\left(\frac{\alpha_\mu\theta_P}{1+\theta_P}\right);\quad \alpha_\mu=\frac{E_\mu}{R_gT_0} \tag{5g}$$

$$S=\frac{\mathfrak{D}_S(T_P,0)}{\mathfrak{D}_{S0}}=\exp\left(\frac{\alpha_S\theta_P}{1+\theta_P}\right);\quad \alpha_S=\frac{E_S}{R_gT_0} \tag{5h}$$

$$B=\frac{b(T_P)}{b_0}=\exp\left(\frac{-\nu\theta_P}{1+\theta_P}\right);\quad \nu=\frac{(-\Delta H)}{R_gT_0} \tag{5i}$$

We also define the nondimensional parameter η as being the ratio of $\mathfrak{D}_S$ at a fractional coverage of θ to $\mathfrak{D}_S$ at zero coverage. The HIO model (Higashi et al., 1963) is often used to explain the coverage dependence of surface diffusivity, i.e., $\eta=1/(1-\theta)$. This relationship can also be derived using the Darken equation, if the driving force is expressed in terms of chemical potential, rather than concentration, and the equilibrium isotherm is of the Langmuir form. Other functional forms of coverage-dependent diffusivity have also been derived (Kapoor and Yang, 1989; Bhatia and Do, 1991). Expressing $\mathfrak{D}_S$ as a function of both particle temperature and fractional coverage, we have

$$\mathfrak{D}_S(\theta_P,\theta)=\mathfrak{D}_S(0,0)\eta S \tag{5j}$$

In nondimensional form, the microsphere mass balance equation (Eq. 1) becomes:

$$\frac{\partial A_\mu}{\partial \tau}=\gamma P\,\frac{1}{x_\mu^2}\,\frac{\partial}{\partial x_\mu}\left(x_\mu^2\,\frac{\partial A_\mu}{\partial x_\mu}\right) \tag{6}$$

with boundary conditions,

$$x_\mu=0;\quad \frac{\partial A_\mu}{\partial x_\mu}=0 \tag{6a}$$

$$x_\mu=1;\quad A_\mu=\frac{(1+\lambda)BA}{(1+\lambda BA)} \tag{6b}$$

and the particle equation (Eq. 2) becomes:

$$\sigma_1\,\frac{\partial A}{\partial \tau}+\sigma_2\,\frac{\partial \overline{A}_\mu}{\partial \tau}=Q\,\frac{1}{x^s}\,\frac{\partial}{\partial x}\left(x^s\,\frac{\partial A}{\partial x}\right)$$
$$+\delta S\left[\frac{\eta}{x^s}\,\frac{\partial}{\partial x}\left(x^s\,\frac{\partial \overline{A}_\mu}{\partial x}\right)+\frac{\partial \eta}{\partial x}\,\frac{\partial \overline{A}_\mu}{\partial x}\right] \tag{7}$$

with boundary conditions,

$$x=0;\quad \frac{\partial A}{\partial x}=\frac{\partial \overline{A}_\mu}{\partial x}=0 \tag{7a}$$

$$x=1;\quad Q\,\frac{\partial A}{\partial x}\bigg|_1+\delta S\left[\eta\,\frac{\partial \overline{A}_\mu}{\partial x}\right]\bigg|_1=Bi(A_b-A|_1) \tag{7b}$$

and the particle heat equation (Eq. 4) is recast in nondimensional form as:

$$\sigma_1\,\frac{d\theta_P}{d\tau}+(s+1)LeBi_h\theta_P$$
$$-\sigma_1\psi(s+1)\int_0^1\left(3\gamma P\,\frac{\partial A_\mu}{\partial x_\mu}\bigg|_1\right)x^s dx=0 \tag{8}$$

Where, for adsorption, the initial condition is:

$$\tau=0;\quad A=A_\mu=0,\quad A_b=1,\quad \theta_P=0 \tag{9a}$$

while for desorption, the initial condition is:

$$\tau=0;\quad A=A_\mu=1,\quad A_b=0,\quad \theta_P=0 \tag{9b}$$

The physical significance of each of the nondimensional parameters is as follows. The parameter σ_1 is the nondimensional macropore capacity (usually $\simeq 0$ for strongly adsorbing systems), while σ_2 is the nondimensional microsphere capacity (usually $\simeq 1$). Gamma (γ) is a measure of the relative diffusion rates in the micropore and in the macropore. Macropore diffusion controls the sorption dynamics when $\gamma \gg 1$, while micropore diffusion controls the dynamics when $\gamma \ll 1$. Delta (δ) is the ratio of surface to macropore diffusional fluxes, where for a system (ignoring the effect of micropore resistance) with macropore diffusion totally controlling the sorption dynamics $\delta = 0$, but for a surface-diffusion-controlled system $\delta > 1$. Lambda (λ) is a measure of the isotherm nonlinearity (the isotherm is linear, nonlinear, and rectangular for $\lambda \simeq 0$, $\lambda \simeq 1$, and $\lambda \gg 1$, respectively). Psi (ψ) is the heat released by sorption in the particle, the Biot number (Bi) is the ratio of the macropore diffusion time to the external film diffusion time, $LeBi_h$ (Lewis-Biot number for heat transfer) is the ratio of macropore diffusion time to external stagnant film heat transfer time, and Q, P, S and B are the temperature-dependent factors for macropore, micropore and surface diffusivity and the Langmuir equilibrium constant, respectively. This nonisothermal formulation is similar to the theoretical model of Sun and Meunier (1987), except that our model allows for the additional coverage-dependent surface flux and neglects the heat transfer resistance in the interior of the particle.

Model equations (Eqs. 6, 7 and 8) were reduced to ordinary differential equations using the orthogonal collocation technique (Villadsen and Michelsen, 1978) and then numerically integrated using an ODE (ordinary differential equation) solver. This computer model was then used to fit the model equations to experimental fractional uptake (mass adsorbed at time t divided by that at equilibrium) data in the time domain. Using 11 collocation points in the particle and five points in the microsphere, typical computation times (depending on the parameter values) were 60-120 seconds for an Intel 20MHz 80386/80387-based computer.

Experimental Studies

The adsorption equilibrium capacity and the adsorption dynamics of CO_2 on an Ajax commercial high-surface area carbon (Norit RB) were determined using an electronic microbalance. Full details of the carbon properties and the experimental technique were published earlier (Gray and Do, 1989). To vary the values of the model parameters γ and δ, the sorption dynamics were measured over a range of particle sizes ($R = 0.1$-0.3 cm) and geometries (slab and cylinder), sorbate gas concentrations (2.0-50 mol % CO_2 in helium) and particle temperatures (25-150°C). Cylindrical and slab geometry particles were made by sealing appropriate sides of the carbon extrudates with epoxy resin.

A high sorbate gas velocity was used to make the sorption conditions during dynamic runs differential (i.e., constant sorbate concentration surrounding the sorbent particle, and minimized external mass and heat transfer resistance), thus making C_b in Eq. 2b a constant. The values of the Biot and $LeBi_h$ numbers in Eq. 5e were calculated using the Ranz-Marshall correlation for single particles (Wakao and Kaguei, 1982). Under these experimental conditions typical values of the model parameters were: $\lambda = 0.1$-1, $\gamma = 1$-10, $\delta = 0.5$-1, $\sigma_1 = 0(0.01)$, $\psi = 0.05$-0.1, $Bi = 50$-100, and $LeBi_h = O(0.05)$.

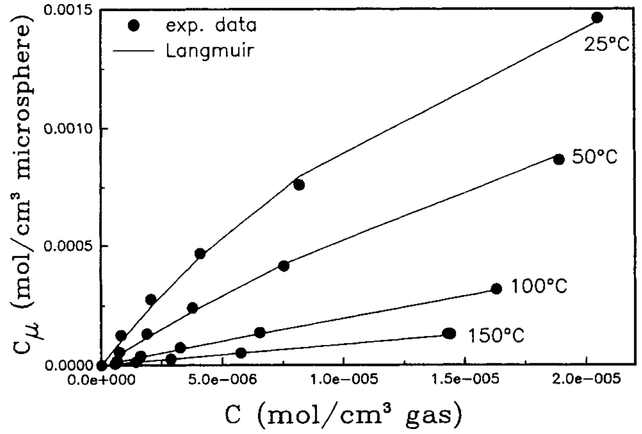

Figure 1. Carbon dioxide adsorption isotherms on Ajax activated carbon.

Results and Discussion

Sorbent equilibrium capacity

The experimentally-determined equilibrium capacity of carbon dioxide on the Ajax activated carbon is shown in Figure 1. The Langmuir equation was fitted to the data over all concentrations and temperatures, while keeping $C_{\mu s}$ (adsorbed-phase saturation concentration) constant. The Langmuir isotherm fitted the data quite well, and the values of the constants b and $C_{\mu s}$ in the isotherm (Eq. 1b) were obtained as shown in Table 1. While any form of isotherm may be used in the dynamic model, the Langmuir isotherm was used as it best fitted the experimental data. The heat of adsorption ($-\Delta H$) was determined by fitting the Langmuir isotherm equilibrium constant (b) to the van't Hoff equation, from which the heat of adsorption ($-\Delta H$) was calculated to be 22.2 kJ/mol (5.31 kcal/mol). Andrieu and Smith (1980) determined ($-\Delta H$) of 6.0 kcal/mol for CO_2 on BPL activated carbon, although their value was the isosteric heat of adsorption at zero coverage. The ($-\Delta H$) extracted from our experimental capacity data was then used to calculate the parameter ψ.

Adsorption dynamics

The theoretical model has three dynamic fitting parameters ($\mathfrak{D}_{P0}$, $\mathfrak{D}_{S0}$ and $\mathfrak{D}_o/R_\mu^2$), although for these experimental data only two ($\mathfrak{D}_{S0}$ and $\mathfrak{D}_0/R_\mu^2$) were used. We did not need to use $\mathfrak{D}_{P0}$ as a fitting parameter, as it was calculated *a priori* from the composite diffusivity ($\mathfrak{D}_M$) and the previously determined tortuosity factor for Ajax carbon of $\tau_M = 8.0$ (Gray and Do, 1990), i.e., $\mathfrak{D}_{P0} = \mathfrak{D}_M/\tau_M$. Furthermore, the temperature-dependency factor (β in Eq. 5f) for $\mathfrak{D}_{P0}$ was determined to be

Table 1. Values of Langmuir Isotherm Constants at Various Temperatures

Temp. (°C)	b (cm³Gas/mol)	$C_{\mu S}$ (mol/cm³ Microsphere)
25	40.6×10^3	0.00319
50	20.3×10^3	"
100	6.70×10^3	"
150	2.87×10^3	"

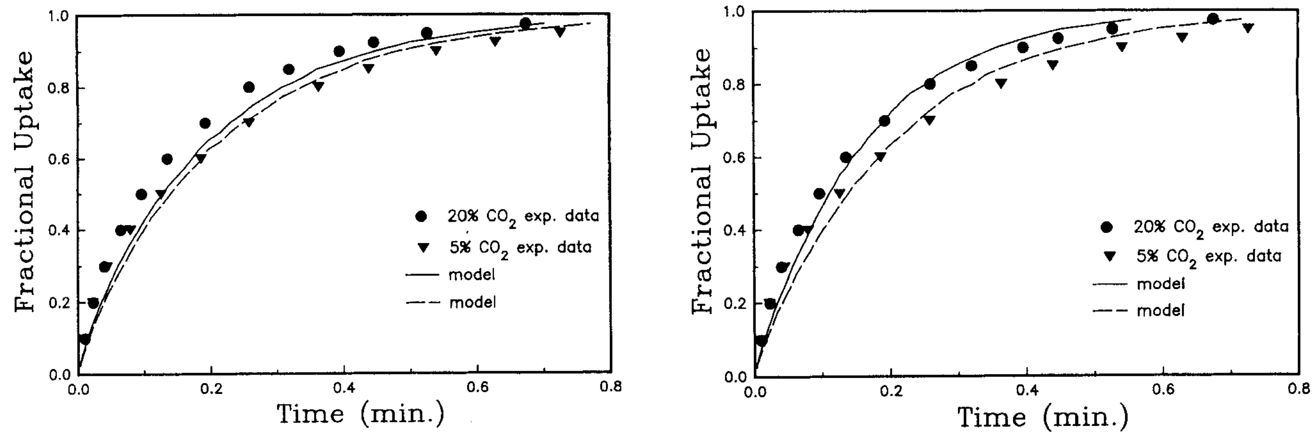

(a) Constant surface diffusivity

(b) Surface diffusivity dependent on coverage

Figure 2. Model adsorption uptake fitted to experimental data with various CO_2 concentrations on 0.1-cm radius slab at 25°C

Parameters: 5% CO_2, $\lambda = 0.083$, $\gamma = 1.3$, $\delta = 0.80$; 20% CO_2, $\lambda = 0.33$, $\gamma = 1.0$, $\delta = 0.65$

1.25, calculated from the temperature dependency of molecular and Knudsen diffusion.

The experimental data for CO_2 adsorption, at various concentrations and temperatures, on 0.1- and 0.3-cm-radius carbon slabs were fitted with the model to determine the surface and micropore diffusivities ($\mathcal{D}_{S0}$ and $\mathcal{D}_0/R_\mu^2$). In the first instance, surface diffusivity was assumed to be independent of coverage ($\eta = 1$), and this model fits the experimental adsorption uptake curves over a range of temperatures (with concentration held constant) quite well. However, as shown in Figure 2a, the simplified model does not adequately fit uptake curves over a range of concentrations (with temperature held constant): at the higher concentration levels (20% CO_2), the model predicts slower uptake than observed experimentally. If the adsorption isotherm is significantly nonlinear (favorable), the adsorption dynamics will accelerate as the gas-phase concentration is increased. However, the value of λ (Langmuir isotherm parameter, Eq. 5b) for our data is less than 1 ($\lambda = 0.33$ for 20% CO_2, 25°C), so the isotherm is not highly nonlinear, and the nonlinearity effect can therefore account only for a rather moderate increase in uptake rate with CO_2 concentration. Since the faster experimental uptake rate with 20% CO_2 cannot be explained as an isotherm effect, we concluded that the effect is probably due to an increase in surface diffusivity with coverage.

The surface diffusivity, in the model, was therefore allowed to vary with coverage according to the HIO model (Higashi et al., 1963) or Darken equation, i.e., $\eta = 1/(1-\theta)$. However, this gave only a marginal improvement in the fit. Apart from the HIO treatment, several other models have been proposed to explain the concentration dependence of surface diffusion. A recent model by Bhatia and Do (1991), in which diffusion is modeled by the random walk formulation of Bhatia (1986), showed that surface diffusion coefficients are affected strongly by structural heterogeneity (i.e., nonuniform pore-size distribution) and increase more strongly with sorbed concentration than would be predicted by the Darken equation. The parameters in this model are specific to each sorbate/sorbent system and are obtained by integrating a pore-size-dependent Langmuir isotherm over the sorbent pore-size distribution.

The method of Bhatia and Do (1991) was applied to our CO_2/activated-carbon system to determine the coverage dependency of the surface diffusion coefficient. The resulting ratio, $\mathcal{D}_S(0,\theta)/\mathcal{D}_S(0,0)$, is plotted against the fractional coverage ($\theta = C_{\mu 0}/C_{\mu s}$) in Figure 3. As can be seen from this figure, the surface diffusivity (for the Bhatia and Do model) depends more strongly on coverage than would be predicted by the Darken equation, even at the relatively low concentrations used in our experiments (e.g., $\theta = 0.25$ for 20% CO_2 at 25°C). Using this stronger concentration-dependent surface diffusivity, the dynamic adsorption uptake model was refitted to the experimental data, Figure 2b, where the fit is much better than the corresponding curves of Figure 2a (no coverage dependence). One can apply the Darken equation to isotherms other than the Langmuir form and obtain a stronger thermodynamic factor (coverage dependence) for surface diffusivity, e.g., the Volmer isotherm gives $\eta = 1/(1-\theta)^2$. However, we found that the model of Bhatia and Do (1991) provided the best prediction of coverage-dependent diffusivity for our data.

The effect of temperature on the nondimensional adsorption uptake of 20% CO_2 on a 0.3-cm slab is shown in Figure 4a,

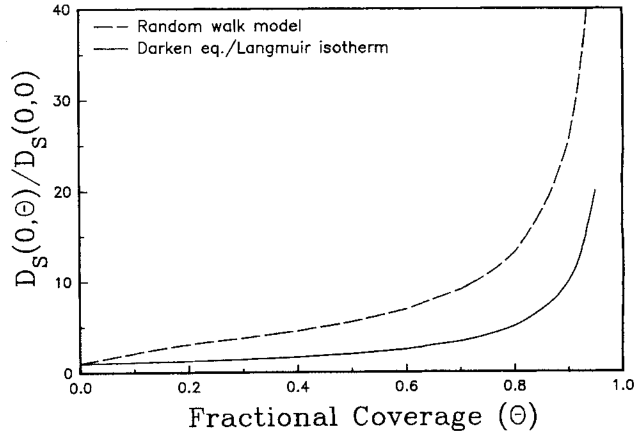

Figure 3. Coverage dependence of surface diffusivity according to random walk model (Bhatia and Do, 1991) and Darken equation applied to Langmuir isotherm.

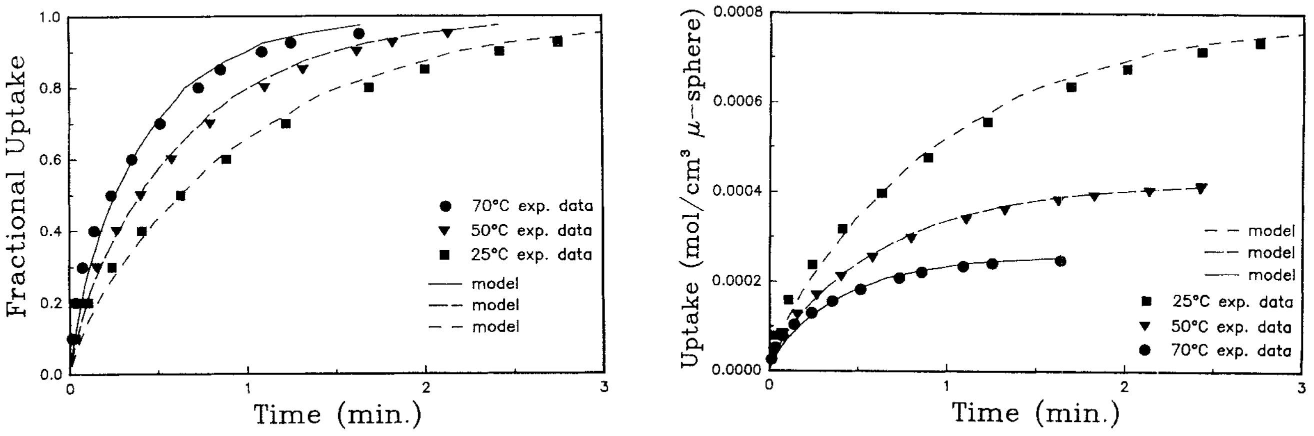

(a) Nondimensional uptake

(b) Dimensional uptake

Figure 4. Model adsorption uptake fitted to experimental data at various temperatures on 0.3-cm radius slab with 20% CO_2.

Parameters: 25°C, $\lambda=0.33$, $\gamma=9.3$, $\delta=0.65$; 50°C, $\lambda=0.15$, $\gamma=6.4$, $\delta=0.61$; 70°C, $\lambda=0.089$, $\gamma=4.6$, $\delta=0.59$

where the model fits the data quite well. This same dynamic data can also be expressed as dimensional (real) uptake vs. time as shown in Figure 4b, where it is observed that the order of the curves is opposite to that in Figure 4a, i.e., the lower temperature curves appear faster. However, the true effect of temperature on the adsorption dynamics is observed by normalizing the uptake curves by their respective mass adsorbed at equilibrium (thus, removing the capacity effect), which is how the data are expressed in Figure 4a. The values of the diffusion coefficients extracted at each temperature are given in Table 2.

The diffusivities shown in Table 2 were obtained using particle sizes of 0.1- and 0.3-cm radius slabs. The ability of the model to predict the effect of varying particle size/geometry is shown by simulations in Figure 5, in which model predictions (using diffusivities from Table 2) are compared with the experimental data for adsorption at 25°C of 20% CO_2 on 0.1-cm cylinder and 0.2-cm slab particles, as well as on the original 0.1-cm and 0.3-cm slab particles. The reasonably good fit of the model prediction uptake curves to the experimental data lends support to the validity of our theoretical model.

The macropore and micropore diffusivities from our data are of the same order of magnitude to those of Andrieu and Smith (1980), although our macropore and micropore diffusivities were smaller than theirs. This discrepancy is not unexpected, since the structural properties as well as the model of Andrieu and Smith's carbon (BPL) were different from ours (they did not include a surface-diffusion mechanism). The surface diffusivities from our data are also of the same order as the results of Popielawski (1967). The values of $\mathfrak{D}_0/R_\mu^2$ and $\mathfrak{D}_{S0}$ extracted at each temperature (Table 2) were fitted to an Arrhenius expression to give an activation energy for micropore diffusivity of $E_\mu = 8.4$ kJ/mol (2.0 kcal/mol) and for surface diffusivity of $E_S = 19.7$ kJ/mol (4.7 kcal/mol). As expected, the value of E_S is similar to, but less than, the heat of adsorption, while the value of E_μ is smaller than expected. In all the dynamic adsorption curves experimentally measured in this work, the value of γ was ≥ 1, indicating that the sorption dynamics (ignoring surface diffusion effects) were controlled by macropore resistance ($\gamma \gg 1$) or a combination of macropore and micropore resistance ($\gamma \simeq 1$). As none of the adsorption curves were determined under purely micropore diffusion control ($\gamma \ll 1$), the estimated values of $\mathfrak{D}_0/R_\mu^2$ (at each temperature) have some error, and consequently this error may make the value of E_μ smaller than expected.

Table 2. CO_2 Macropore Diffusivities with $\tau_M = 8.0$, and Surface and Micropore Diffusivities Fitted to Adsorption Data

Temp. (°C)	$\mathfrak{D}_{PO}$ (cm²/s)	$\mathfrak{D}_{S0}$ (cm²/s)	$\mathfrak{D}_0/R_\mu^2$ (1/s)
25	0.047	1.4×10^{-4}	0.022
50	0.052	2.5×10^{-4}	0.029
70	0.056	4.0×10^{-4}	0.034

Particle temperature rise

The temperature rise in the particle, due to the heat released by adsorption, was determined both experimentally and from

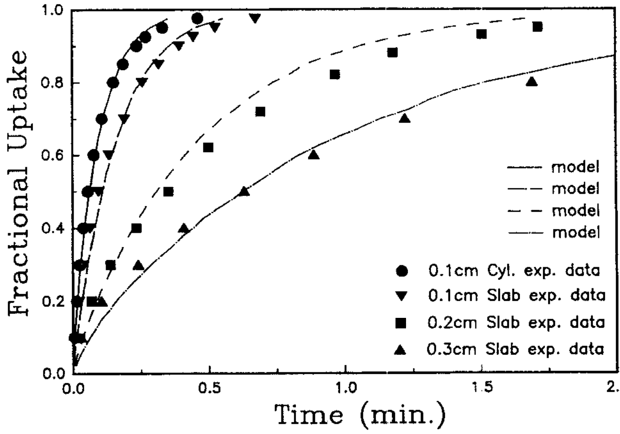

Figure 5. Model simulation adsorption uptake compared to experimental data with various particle sizes at 25°C and 20% CO_2.

Parameters: $\lambda=0.33$, $\delta=0.65$; R=0.1-cm cylinder and slab, $\gamma=1.0$; R=0.2-cm slab, $\gamma=4.1$; R=0.3-cm slab, $\gamma=9.3$

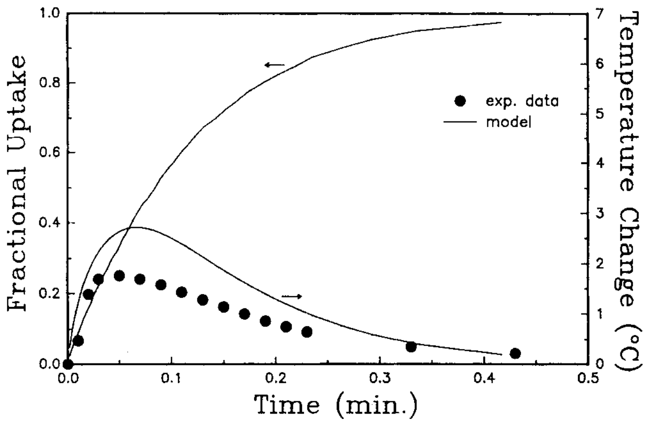

Figure 6. Particle experimental temperature rise and predicted uptake and temperature dynamics for adsorption of 50% CO_2 on 0.1-cm radius slab at 25°C.

Model parameters: $\lambda = 0.83$, $\gamma = 0.75$, $\delta = 0.47$, $\psi = 0.11$

the model. To measure the particle temperature rise, a minute type T thermocouple junction (made from 0.025-mm copper and constantan wires) was embedded in a 0.1-cm radius slab carbon particle. This particle was then suspended in the microbalance apparatus in the same configuration, as was used for the sorption dynamic experiments, and contacted with 50% CO_2 at 25°C. The model simulation of the particle temperature took into account the thermal mass of epoxy resin surrounding the carbon particle and the heat loss through the epoxy layer. The measured temperature rise and the model simulation particle temperature and uptake dynamics are shown in Figure 6. The experimentally-determined particle temperature variation with time has the same shape as the theoretically-predicted curve, but is a little smaller in magnitude. This is probably due to: (1) imperfect contact between the thermocouple and the carbon particle; (2) heat conduction along the thermocouple leads; and (3) error in estimating the heat transfer coefficient from the Ranz-Marshall correlation (low Reynolds number). While the temperature rise for our CO_2/carbon system is not excessive, the inclusion of the energy balance (Eq. 8) makes the dynamic model generally applicable to adsorbate/adsorbent systems where heat transfer resistance is more significant.

Effect of experimental conditions on model parameters

Examination of the variation in the nondimensional dynamic parameters (γ and δ) helps to explain what is happening in the sorbent particle as experimental conditions are altered. The effect of temperature on γ (the ratio of macropore to micropore diffusional resistance) can be observed in Figure 4a (20% CO_2, 0.3-cm slab), where γ decreases from 9.3 at 25°C to 4.6 at 70°C. The three temperature-dependent factors of γ (Eq. 5d) are $C_{\mu 0}/C_0$, $\mathfrak{D}_0$ and $\mathfrak{D}_{P0}$, and of these factors $C_{\mu 0}/C_0$ has the strongest temperature dependency, as the heat of adsorption $(-\Delta H)$ is much greater than the micropore diffusion activation energy (E_μ) or the macropore diffusion temperature coefficient (β). As a result, when the temperature is increased, the decrease in $C_{\mu 0}/C_0$ more than compensates for the increase in $\mathfrak{D}_0$ and $\mathfrak{D}_{P0}$, so that γ decreases and micropore resistance becomes relatively more important. The effect of particle size on γ is straightforward, with macropore resistance and γ increasing according to particle radius squared (Eq. 5d), as shown in Figure 5.

The ratio of surface to macropore flux is represented by δ (Eq. 5d); however, we now define two new terms to show the fraction of the total flux contributed by the macropore and by the surface flux. These terms are δ_1, the nondimensional macropore flux, and δ_2, the nondimensional surface flux. These terms are expressed as:

$$\delta_1 = \frac{\epsilon_M \mathfrak{D}_{P0}}{[\epsilon_M \mathfrak{D}_{P0} + (1-\epsilon_M)\mathfrak{D}_{S0} C_{\mu 0}/C_0]} = \frac{1}{(\delta+1)}; \quad \delta_2 = 1 - \delta_1 \tag{10}$$

The effect of temperature (at constant sorbate concentration, 20% CO_2) on the fluxes can be seen in Figure 4a, where the ratio of surface to macropore flux (δ) decreases from 0.652 at 25°C to 0.588 at 70°C. Consequently, the nondimensional surface flux (δ_2) decreases from 40% at 25°C to 37% at 70°C. This trend is to be expected since, when the heat of adsorption $(-\Delta H)$ is larger than the activation energy of surface diffusion (E_S), $C_{\mu 0}/C_0$ decreases more substantially than when $\mathfrak{D}_{S0}$ increases with an elevated temperature.

Conclusions

The single-particle theoretical model in this article describes the adsorption dynamics of CO_2 on the activated carbon based on the mechanisms of macropore, micropore and surface diffusion. The adsorption equilibrium was described by a Langmuir isotherm, and the effects of particle nonisothermality and coverage dependence of the surface diffusivity were also included. Using a particle tortuosity factor of $\tau_M = 8.0$ (determined in a previous work), the macropore diffusivity was calculated to be 0.047 cm^2/s at 25°C. Fitting the model to gravimetrically-measured data gave surface and micropore diffusivities of 1.4×10^{-4} cm^2/s and 0.022 s^{-1}, respectively, at 25°C. These diffusivities are of the same order as values determined by other workers for CO_2 on the activated carbon. The heat of adsorption and activation energies for micropore and surface diffusivity were 22.2, 8.4 and 19.7 kJ/mol, respectively. While the heat of adsorption and the surface diffusivity activation energy obtained were reasonable values, the value of the micropore diffusivity activation energy was lower than expected.

Apart from the diffusion mechanisms, two other effects were found to be involved: coverage dependence of the surface diffusivity and temperature rise of the particle. The surface diffusivity was found to depend more strongly on coverage than was predicted by applying the Darken equation to the Langmuir isotherm. However, a model with surface diffusion coefficients strongly affected by sorbent structural heterogeneity (Bhatia and Do, 1991) predicted adequately the coverage dependency of our data. The temperature rise of the particle due to heat released by adsorption was measured experimentally and predicted by the model. Although the particle was nonisothermal, the increase in temperature was not excessive.

Acknowledgment

We would like to thank Professors S. K. Bhatia and D. M. Ruthven for their advice and assistance with this research. Financial support for this work was provided by the Australian Research Council.

Notation

A = dimensionless macropore concentration $= C/C_0$
A_μ = dimensionless microsphere concentration $= C_\mu/C_{\mu 0}$
$\overline{A_\mu}$ = dimensionless average microsphere concentration $= \overline{C_\mu}/C_{\mu 0}$
A_b = ratio of bulk concentration to initial concentration $= C_b/C_0$
B = parameter in dimensionless Langmuir isotherm
Bi = Biot number
b = constant in Langmuir isotherm, cm^3/mol
C = macropore concentration, mol/cm^3 gas
C_0 = initial macropore concentration, mol/cm^3 gas
C_b = bulk gas phase concentration, mol/cm^3 gas
C_μ = microsphere concentration, mol/cm^3 microsphere
$\overline{C_\mu}$ = average microsphere concentration, mol/cm^3 microsphere
$C_{\mu 0}$ = sorbed concentration in equilibrium with C_0, mol/cm^3 microsphere
$C_{\mu S}$ = maximum sorbed phase concentration in Langmuir isotherm
C_P = particle heat capacity, J/g·K
$\mathcal{D}_{AB}$ = molecular diffusivity (gas-phase), cm^2/s
$\mathcal{D}_e$ = effective diffusivity, cm^2/s
$\mathcal{D}_K$ = Knudsen diffusivity, cm^2/s
$\mathcal{D}_M$ = composite molecular diffusivity $= (1/\mathcal{D}_{AB} + 1/\mathcal{D}_K)^{-1}$, cm^2/s
$\mathcal{D}_P$ = particle macropore diffusivity $= \mathcal{D}_e/\epsilon_M$, cm^2/s
$\mathcal{D}_S$ = surface diffusivity, cm^2/s
$\mathcal{D}$ = micropore diffusivity, cm^2/s
E_S = surface diffusivity activation energy, kJ/mol
E_μ = micropore diffusivity activation energy, kJ/mol
h = particle external film heat transfer coefficient, W/cm^2·K
$-\Delta H$ = heat of adsorption, kJ/mol
k_m = particle external film mass transfer coefficient, cm/s
$LeBi_h$ = Lewis × Biot (heat) number
P = micropore diffusivity temperature dependency factor
Q = macropore diffusivity temperature dependency factor
r = particle radial coordinate
r_μ = microsphere radial coordinate
R = radius of particle, cm
R_μ = radius of microsphere, cm
R_g = gas constant, J/mol·K
s = particle shape factor (0 = slab, 1 = cylinder, 2 = sphere)
S = surface diffusivity temperature dependency factor
T_P = particle temperature, K
t = real time coordinate
x = dimensionless particle radial coordinate $= r/R$
x_μ = dimensionless microsphere radial coordinate $= r_\mu/R_\mu$

Greek letters

α_μ = nondimensional micropore diffusion activation energy
α_S = nondimensional surface diffusion activation energy
β = temperature coefficient of macropore diffusivity
δ = ratio of sorbed phase to macropore flux
ϵ_M = macropore porosity
η = coverage dependency factor of surface diffusion
γ = ratio of macropore to micropore diffusional resistance
λ = Langmuir isotherm nonlinearity parameter
ν = nondimensional heat of adsorption
ρ_P = particle density, g/cm^3
ψ = nondimensional heat released by adsorption
σ_1 = nondimensional macropore capacity
σ_2 = nondimensional microsphere capacity
θ_P = lumped particle temperature
θ = fractional coverage $= C_\mu/C_{\mu S}$ for a Langmuir isotherm
τ = nondimensional time
τ_M = macropore tortuosity factor $= \epsilon_M \mathcal{D}_M/\mathcal{D}_e = \mathcal{D}_M/\mathcal{D}_P$

Subscripts

0 = initial or equilibrium condition

Literature Cited

Andrieu, J., and J. M. Smith, "Rate Parameters for Adsorption of CO_2 in Beds of Carbon Particles," *AIChE J.*, **26**, 944 (1980).

Ash, R., R. M. Barrer, and C. G. Pope, "Flow of Adsorbable Gases and Vapours in a Microporous Medium: I. Single Sorbates," *Proc. Roy. Soc. A*, **271**, 1 (1963).

Bhatia, S. K., "Stochastic Theory of Transport in Inhomogeneous Media," *Chem. Eng. Sci.*, **41**, 1311 (1986).

Bhatia, S. K., and D. D. Do, "On the Concentration Dependence of Surface Diffusion Coefficients in Capillary Porous Materials," *Proc. Roy. Soc.*, in press (1991).

Carman, P. C., and F. A. Raal, "Diffusion and Flow of Gases and Vapours through Micropores: III. Surface Diffusion Coefficients and Activation Energies," *Proc. Roy. Soc. A*, **209**, 38 (1951).

Doong, S. J., and R. T. Yang, "Bulk Separation of Multicomponent Gas Mixtures by Pressure Swing Adsorption: Pore/Surface Diffusion and Equilibrium Models," *AIChE J.*, **32**, 397 (1986).

Gray, P. G., and D. D. Do, "Adsorption and Desorption of Gaseous Sorbates on a Bidispersed Particle with Freundlich Isotherm: II," *Gas Sep. Purif.*, **3**, 201 (1989).

Gray, P. G., and D. D. Do, "Adsorption and Desorption of Gaseous Sorbates on a Bidispersed Particle with Freundlich Isotherm: III," *Gas Sep. Purif.*, **4**, 149 (1990).

Gregg, S. J., and K. S. W. Sing, *Adsorption, Surface Area and Porosity*, Academic Press, London (1982).

Higashi, K., H. Ito, and J. Oishi, "Surface Diffusion Phenomena in Gaseous Diffusion: I. Surface Diffusion of Pure Gas," *J. Atomic Energy Soc. Japan*, **5**, 846 (1963).

Kapoor, A., and R. T. Yang, "Surface Diffusion on Energetically Heterogeneous Surfaces," *AIChE J.*, **35**, 1735 (1989).

Popielawski, J., "The Surface Flow of Adsorbed Carbon Dioxide on Active Carbon," *J. Catal.*, **7**, 263 (1967).

Ruthven, D. M., *Principles of Adsorption and Adsorption Processes*, Wiley, New York (1984).

Sircar, S., "Sorption of Carbon Dioxide on Activated Carbons: Effect of the Heat of Sorption during Kinetic Measurements," *Carbon*, **19**, 153 (1981).

Sun, L. M., and F. Meunier, "Nonisothermal Adsorption in a Bidisperse Adsorbent Pellet," *Chem. Eng. Sci.*, **42**, 2899 (1987).

Villadsen, J., and M. L. Michelsen, *Solution of Differential Equation Models by Polynomial Approximation*, Prentice-Hall, Englewood Cliffs, NJ (1978).

Wakao, N., and S. Kaguei, *Heat and Mass Transfer in Packed Beds*, Gordon and Breach, New York (1982).

Yang, R. T., *Gas Separation by Adsorption Processes*, Butterworths, Boston (1987).

Yucel, H., and D. M. Ruthven, "Diffusion of CO_2 in 4A and 5A Zeolite Crystals," *J. Coll Interf. Sci.*, **74**, 186 (1980).

Manuscript received Aug. 28, 1990, and revision received May 17, 1991.